JOURNAL OF CATALYSIS 156, 279–289 (1995)

Carbon-Supported and Alumina-Supported Niobium Sulfide Catalysts

Nabil Allali,* Anne-Marie Marie,* Michel Danot, Christophe Geantet,† and Michèle Breysse†,[1]

*Laboratoire de Chimie des Solides, IMN-CNRS, UMR 0110, Université de Nantes, 2 Rue de la Houssinière, 44072 Nantes Cédex 03, France; and †Institut de Recherches sur la Catalyse, CNRS, 2 Avenue Albert Einstein, 69626 Villeurbanne Cédex, France

Received November 18, 1994; revised May 24, 1995; accepted June 29, 1995

Few studies deal with the properties of niobium sulfide as a hydrodesulfurization catalyst. In this paper, the preparation of carbon-supported niobium sulfide catalysts was optimized concerning (i) the nature of the soluble precursor, (ii) the drying process, and (iii) the sulfurizing treatment, which was always performed under atmospheric pressure but for different H_2S-based flows and reaction temperatures. The activities of the best samples prepared with niobium oxalate as the impregnation salt, drying at room temperature, and presulfurization with N_2/H_2S at 400°C are superior to that of a supported MoS_2 reference catalyst. Alumina-supported systems can be sulfurized only under more severe conditions (CS_2 under pressure). After optimization of the sulfurization treatment (400°C, 10 h) the maximum activity obtained is significantly higher than that of a molybdenum sulfide reference catalyst. The catalytic activities of the various catalysts studied are related to their morphological and chemical characteristics using TPR and EXAFS measurements. The work illustrates the importance of the support and the sulfurization method on the genesis of a niobium sulfide active phase. © 1995 Academic Press, Inc.

INTRODUCTION

Considering the increasingly drastic regulations concerning the emission of SO_x and NO_x gases, conventional alumina-supported CoMo, NiMo, and NiW sulfide hydrotreating catalysts will not be effective enough for heteroatom removal. This opens up a challenge for the development of new catalysts. Systematic studies performed on unsupported catalysts have revealed that other sulfides such as RuS_2 or niobium sulfides may be useful substitutes (1, 2), with niobium having the advantage of a low price.

In comparison with other sulfides, only a few studies have dealt with niobium sulfides as catalysts. Lewis and Kenney first reported their application for the isomerization and hydrogenation of 1-butene in the presence of H_2S (3). Later, unsupported samples of niobium trisulfide and disulfide were used as model catalysts for characteristic hydrotreating reactions (4–6). Niobium disulfide NbS_2 exhibits the same overall structural features as MoS_2, i.e., a lamellar arrangement of trigonal prisms [NbS_6]. In contrast, the structure of niobium trisulfide NbS_3 is completely different, even though it is built from the same [NbS_6] prismatic units. In NbS_3, these prisms share their triangular faces to constitute infinite "fibers," which are associated due to interfiber Nb–S bonds and they form corrugated slabs (5–7). In these slabs the atomic arrangement is much more complicated than in those of disulfides. The electronic structure of NbS_3 is rather original too, with anion and cation pairing. The formula can be written as $Nb^{4+}S^{2-}(S_2)^{2-}$, with sulfur pairs $(S_2)^{2-}$ similar to those present in pyrite structures. In addition, the d^1 electrons of niobium are associated in Nb–Nb bonds (5). Compared to MoS_2 and WS_2, unsupported niobium sulfides (especially the trisulfide NbS_3) present higher activities. In particular, they show interesting potentialities for hydrogenation reactions and good performances in the presence of H_2S in contrast with conventional catalysts. Moreover, they present a particular ability to perform C–C and C–N bond cleavage (8).

Concerning supported niobium sulfide systems applied to hydrotreatment, the literature is scarce and often contradictory. In a screening work performed by Ledoux *et al.* (9), niobium sulfide supported at low concentration on carbon presented a low HDS activity. Mixed systems were also studied and a synergistic effect was found in HDS model reaction for sulfurized Ni–Nb/SiO_2 catalysts (10). In the same system, Hillerova *et al.* (11) did not observe this effect. Recently, we demonstrated that niobium sulfide supported on carbon is particularly efficient for the reactions of scission of carbon–nitrogen bonds (6), as already reported for the unsupported samples. The discrepancies between the various results reported suggest that the catalytic characteristics of the supported niobium sulfide systems are closely related to the synthesis parameters. The transposition to the supported state is a crucial point for the elaboration of new catalytic systems. Precise study of

[1] To whom correspondence should be addressed at Institut de Recherches sur la Catalyse, 2 Avenue Albert Einstein, 69626 Villeurbanne Cédex, France. Fax: (33) 72 44 53 99. E-mail: geantet@catalyse.univ-lyon1.fr

0021-9517/95 $12.00

the role of the preparation parameters must be conducted, since for instance the choice of the precursor salt and support may be determinative.

Another major aspect of the development of new supported systems concerns the sulfurization, or activation, procedure. A large variety of sulfurizing agents such as hydrogen sulfide, carbon disulfide, dimethyldisulfide (DMDS), pure organic compounds, and mixtures of sulfur-containing molecules present in pretroleum fractions may be used. In practice, there is no standard protocol of activation but DMDS is often used in the industrial context and mixtures of H_2/H_2S on the laboratory scale. The activating molecule may greatly influence the catalytic properties: Prada Silvy *et al.* observed differences in catalytic activity on CoMo catalysts (12), and selectivity can also be influenced in such classical systems (13). More drastic changes were observed on Ru-based systems. The presence of hydrogen induces an important sintering whereas a N_2/H_2S mixture provides well-dispersed catalysts with high HDS activities (14). Similar effects were found on mixed systems such as RuMo or NiRu sulfides supported on alumina (15, 16). After the sulfurizing agent has been chosen, the sulfurization conditions (temperature and duration) must be optimized.

The purpose of the present work was the transposition of niobium sulfide to the supported state, i.e., the optimization of preparation parameters including sulfurization conditions. In fact, thermodynamic data show that the free energy of sulfurization of niobium oxide is positive and clearly indicate that this reaction should be not easy compared to that of Mo or W oxides (17). Moreover, the calcination step of niobium oxide should be avoided, to hinder good crystalline organization.

For our first attempts we chose oxide supports: alumina and silica. On these supports and using conventional sulfurizing treatments (H_2S-based flows under atmospheric pressure) significant sulfurization can be obtained only at high temperature (800°C) (18). Under these conditions, sintering of the formed niobium sulfide occurs, which results in very low catalytic activities. Such difficulties in sulfurizing niobium on oxide supports can be attributed to strong support–cation interactions. Considering these preliminary results, we used two different routes to obtain supported niobium sulfide. First, instead of oxides, we chose carbon as the support, because of the weakness of the interactions which it has with metallic cations. Second, using oxide supports, we carried out the sulfurization treatment under conditions more severe than the conventional ones.

EXPERIMENTAL

Sample Preparation

Supported niobium sulfides were prepared using two supports: carbon and alumina. The supports we chose are "Norit RX3" carbon, with a surface area of 1200 m^2/g and a pore volume of 1 cm^3/g, and a Rhône-Poulenc γ-alumina with a surface area of 256 m^2/g and a pore volume of 0.6 cm^3/g. The optimization of the synthesis represents an important part of the present work and for this reason will be reported in detail in separate sections for each support.

Catalytic Activities

All the catalysts prepared were tested in the thiophene hydrodesulfurization model reaction, under atmospheric pressure at 350°C, using a continuous flow microreactor. The catalyst (about 0.1 g) was introduced into the reactor under an argon atmosphere. The hydrogen flow was saturated with thiophene vapor at 0°C ($P_{\text{thiophene}} = 18$ Torr) and the total flow rate was 50 ml/min. Steady state conversion was achieved after 16 h and the specific rate was determined according to the equation:

$$A(\text{HDS}) = Q \cdot \tau/m \ (\text{mol s}^{-1}\ \text{g}^{-1}),$$

where Q is the thiophene flow rate (mol s^{-1}), τ is the conversion, and m is the weight of the catalyst. The total conversion, τ, was always lower than 15%.

Characterization

Attempts to obtain X-ray diffraction patterns of our carbon-supported samples were unsuccessful, due to a poor crystalline organization. In addition, electron microscopy gave images with very bad contrast. We could, however, characterize these catalysts with the aid of EXAFS (extended X-ray absorption fine structure) and TPR (temperature-programmed reduction) techniques. For some of the alumina-supported catalysts, X-ray diffraction patterns could be obtained using a INEL curved detector and Cu$K\alpha_1$ radiation. However, only one weak and broad line could be observed. For that reason, EXAFS and electron microscopy were also used for the characterization of the alumina-supported samples.

EXAFS study. EXAFS spectra were recorded at the Nb*K*-edge on the EXAFS I spectrometer at LURE, the French Synchrotron Radiation Laboratory, using the DCI storage ring. The monochromator was a Si(331) channel cut. The data were collected in the transmission mode, by measurement of the beam intensities I_0 and I, respectively before and after the sample, using ion chambers with argon fill-gas. Approximately 5-μm-thick samples were prepared with the aid of adhesive tape or by dilution in dehydrated boron nitride. The high energy of the Nb*K*-edge does not allow a precise study of the XANES region to be performed, and thus we only recorded the EXAFS spectra from 18,850 to 19,800 eV, with 3-eV steps and a 1-s accumulation time. The EXAFS results were analyzed according to a well-known procedure (19, 20), using a program chain

written by Bonnin and Frétigny for PC microcomputers. As usual, the radial distribution curves which are presented in this article refer to distance values uncorrected for phase shift, whereas real interatomic distances, i.e., values corrected for phase shift, are given in the text.

TPR study. Temperature-programmed reduction (TPR) is a useful technique for the characterization of sulfide catalysts (21–24). It allows the different sulfur species to be identified and their relative amounts to be estimated. The sample was sulfided *ex situ* and transferred under an argon atmosphere. Then, it was purged under nitrogen at room temperature until no H_2S signal (if any) was detected. The temperature was rapidly increased (2°C/min) under a hydrogen flow (100% H_2) to 1100 K. Under these conditions, complete reduction of the sample was not achieved. The quantity of evolving H_2S, measured by a photoionization detector, was plotted versus temperature. The more strongly sulfur is bonded, the higher will be the temperature at which it will be removed as H_2S. For instance, bulk sulfur will be removed after surface sulfur (at higher temperature). For our supported catalysts, the curves were corrected by subtraction of the support contribution.

Electron microscopy. High-resolution microscopy was performed using a Philips CM30 device operating at 300 kV (spherical aberration Cs = 2 mm, resolution = 2.3 Å). The sample was crushed under an argon atmosphere. One part was dropped in ethanol, fragmented and dispersed by ultrasonication, and set on a carbon grid. The images were recorded close to the Scherzer focus.

RESULTS AND DISCUSSION

The Carbon-Supported Catalysts

Optimization of the Synthesis

Choice of the Soluble Precursor for the Impregnation

Soluble niobium-containing compounds are not very numerous, and some of them are rather difficult to prepare. For the present work, we studied three precursors in order to select the best one, considering the obtained catalytic activity and ease of use.

—Ammonium niobate can be prepared as described by Guerchais and Rohmer (25). The solubility in water is important in order that niobium amounts as high as 15% of the support mass can be obtained with the dry-impregnation technique. However, this preparation is somewhat difficult and the solution slowly decomposes with formation of insoluble hydrated niobium oxide, which means that the impregnation must be done with a freshly prepared solution.

—Niobium pentachloride is a commercial product. It often contains significant amounts of oxide due to its high sensitivity to the atmosphere. It is thus necessary to purify it by sublimation and to handle it in a glove box. It can be dissolved in deoxygenated 1 *M* HCl (under an inert atmosphere), but the solubility is low (4 g of niobium per liter). For that reason, the solution-excess technique was in that case preferred to the dry-impregnation technique.

—Like the pentachloride, commercial niobium oxalate often contains oxide. However, niobium oxalate can be rather easily prepared as described by Krishnamurty and Harris (26). A mixture of commercial niobium oxide Nb_2O_5 and potassium persulfate is fused at high temperature in a platinum crucible and heated until the liquid becomes perfectly clear. After cooling, a glassy solid is obtained. After it is carefully ground, it is transferred into a dilute aqueous ammonia solution. Precipitation of hydrated niobium oxide then occurs. The precipitate is filtered, washed with diluted aqueous NH_3 for potassium and sulfate ions to be removed, and dissolved in an oxalic buffer solution. The niobium concentration is determined for 2 ml of the solution: after evaporation at 80°C and calcination at 800°C, the mass of the obtained Nb_2O_5 shows that the amount of niobium is about 10 g per liter. Due to this rather low solubility, the solution-excess technique was also chosen for the impregnation in this case.

TABLE 1

Variation in HDS Activity of Nb/C Sulfide Catalysts (10 wt% of Nb) with the Nature of the Niobium Precursor Compound

Precursor	Niobate	Chloride	Oxalate	Oxalate (TSI)[a]
A(HDS) (10^{-8} mol/s g)	22	40	40	108

[a] TSI: two-step impregnation with 5 wt% of Nb with each step separated by a drying at room temperature.

The activities of catalysts (10 wt% of Nb) obtained from these three precursors, with all the other experimental parameters being exactly similar (*ex situ* sulfidation by N_2/H_2S 15%, flow rate 50 cm^3 min^{-1}, 400°C), were compared in the thiophene hydrodesulfurization model reaction, at 350°C, under atmospheric pressure (Table 1). The sample prepared from ammonium niobate is only half as active as the two other samples, which both present nearly the same activity. The choice thus concerns the oxalate and the chloride. Between them we chose, for all the following syntheses, to use niobium oxalate because, in contrast to the pentachloride, it does not require glove-box handling. For the oxalate precursor and an equivalent total metal loading, we then observed that activity can be improved using a two-step impregnation (5 wt% of Nb each time) separated by a drying at room temperature.

TABLE 2

Variation in HDS Activity of Nb/C Sulfide Catalysts (10 wt% of Nb, Prepared Using the Oxalate Precursor and the Two-Step Impregnation Method) with Sulfurizing Atmosphere

Sulfurizing agent	N_2/H_2S	H_2/H_2S	H_2S
A(HDS) (10^{-8} mol/s g)	110	61	38

The Drying Procedure

After impregnation of the support by the precursor solution, the sample was allowed to dry at room temperature. Higher drying temperatures (e.g., 100°C) cannot be used because niobium cannot then be correctly sulfurized.

Sulfurization Treatment

The sulfurization conditions were varied and the activities of the different samples so obtained were compared in the same reaction as indicated above. All the treatments were carried out under atmospheric pressure, and for 4 h because we never observed any improvement for longer durations.

—Three gas flows were used: $N_2/H_2S(15\%)$, $H_2/H_2S(15\%)$, and pure H_2S. The N_2/H_2S mixture was preferred because if compared to both of the other flows it gives samples which are two to three times more active (Table 2).

—Using this mixture, sulfurization was carried out at T_{sulf} = 350, 400, 500, and 600°C. The sample sulfurized at 400°C has the highest activity (Fig. 1). For T_{sulf} = 350°C no significant activity can be measured, probably because no significant sulfurization occurs. As for the activity decrease observed for T_{sulf} > 400°C, it can be attributed to a sintering of the sulfide particles, as in the case of the alumina-supported samples sulfurized at 800°C (vide supra). However, TPR measurements will show that this is not the only reason (vide infra).

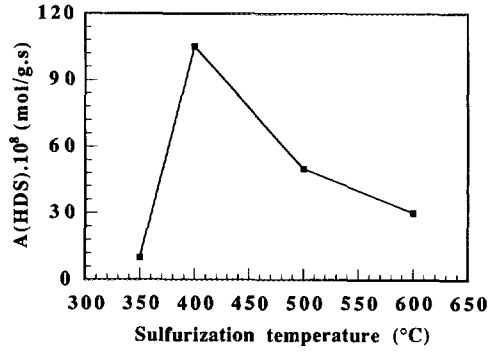

FIG. 1. Variation in the HDS activity of Nb/C sulfide catalysts with the sulfurization temperature.

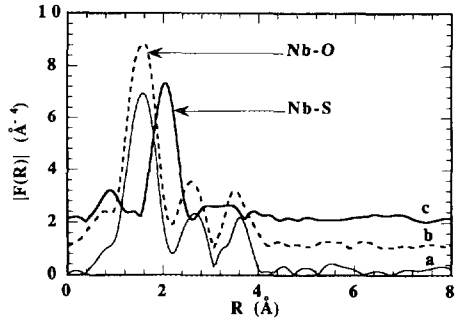

FIG. 2. Radial distribution function obtained at the niobium *K*-edge for (a) the oxalate mother-solution, (b) the sample after impregnation, and (c) the catalyst after sulfurization.

The Niobium Content

Several samples were prepared with different niobium amounts (percentages of the mass of support). The activity increases with the niobium content up to 10% and then remains nearly constant.

Conclusion

The above experiments allowed us to choose for all our syntheses the following conditions:

precursor: niobium oxalate,
niobium amount: 10% of the support mass,
impregnation: solution-excess technique,
drying: at room temperature,
sulfurization treatment: 4 h at 400°C, using N_2/H_2S (15%).

In order to avoid any oxidation, the obtained samples were then handled under an inert atmosphere.

Characterization

EXAFS Results

After impregnation (Fig. 2), the radial distribution function (RDF) is exactly the same as that obtained for the niobium oxalate mother-solution, which means that niobium is deposited on the support as the oxalate. The first peak corresponds to the Nb–O bonds (d_{Nb-O} = 1.95 Å).

After the sulfurization treatment of the carbon-supported catalysts, this peak disappears and is replaced by another one at a higher *R* value (Fig. 2). The corresponding (corrected) distance (2.50 Å) reveals the existence of Nb–S bonds (27). Considering the calculation accuracy (±0.05 Å for such disordered materials), this result cannot be used to establish the nature of the active phase, since the Nb–S distances do not differ much for the various niobium sul-

fides. In fact, for poorly ordered samples, these different phases can be distinguished only by the second peak, which corresponds to Nb–Nb distances (27). In the RDF obtained after sulfurization, a second peak can effectively be observed with possibly two unresolved contributions at about 3.0 and 3.4 Å (uncorrected values). By reference to the RDF obtained for unsupported NbS_2 and NbS_3 (26), these contributions could be attributed to Nb–Nb distances present in NbS_2 and NbS_3, respectively, which could indicate that our catalyst contains NbS_2- and NbS_3-like entities. However, this Nb–Nb peak is very weak, which denotes a very poor crystalline organization. For such disordered systems, the usual calculation programs, which assume a Gaussian distribution of the static component (related to disorder) of the Debye–Waller factor, do not allow reliable values of the structural parameters to be refined. For that reason, we could not calculate the corrected Nb–Nb distances. The existence of this weak peak thus gives a presumption, rather than a proof, of the presence of NbS_2- and NbS_3-like species. However, the EXAFS calculations concerning the first coordination shell clearly establish that sulfurization was achieved.

TPR Study

Three carbon-supported samples were studied, corresponding to different sulfurization temperatures (400, 500, and 600°C). TPR experiments were also devoted to unsupported niobium sulfides for these data to be used as references for the interpretation of the results concerning the catalysts studied. The unsupported sulfides we used for this purpose were NbS_2 and NbS_3 (as prepared from the elements) and NbS_3-D obtained from NbS_3 through a lithium intercalation–deintercalation treatment (5). Due to this treatment, NbS_3-D presents a higher surface area (18 m^2/g) and smaller particle size than NbS_3 (2 m^2/g). Concerning NbS_2, because of the presence of some niobium in the van der Waals space, only a small content of lithium can be intercalated. For that reason, the intercalation–deintercalation treatment has no significant effect on the texture.

The reference NbS_3. The TPR curve of NbS_3 presents three contributions (Fig. 3a), the third one being in fact composed of two poorly resolved peaks. The sulfur losses, and the corresponding temperatures and compositions of the solid, are reported in Table 3. When the S/Nb ratio becomes lower than 2 the X-ray diffraction patterns show that the compounds belong to the $Nb_{1+x}S_2$ structural type (presence of x excess niobium in the van der Waals gap of NbS_2). The corresponding formulae are indicated in parentheses in Table 3.

The first peak is due to the removal of surface sulfur. From the average crystallite dimensions ($1 \times 1 \times 100\ \mu m$) the surface-sulfur/total-sulfur ratio can be estimated to be about 7%, to be compared to the sulfur loss per NbS_3 formula unit (0.14), which corresponds to 5% of the sulfur amount. Taking into account that average crystallite size was used for the calculation, this agreement can be considered satisfactory.

The second contribution leads to the formula $Nb_{1.14}S_2$. Within the experimental accuracy this corresponds to the $NbS_3 \rightarrow Nb_{1.12}S_2$ transition already reported (4, 28). The three following contributions can be related to the removal of bulk sulfur from $Nb_{1.14}S_2$. This removal is far from being complete at the maximum temperature allowed by the experimental device (850°C).

The reference NbS_3-D. The TPR curve of NbS_3-D (Fig. 3a) exhibits the same overall features as that of NbS_3 (Table 3). However, some differences appear. For NbS_3-D, (i) the total quantity of sulfur removed at the end of the experiment is larger; (ii) the first peak, due to surface sulfur, is more important; and (iii) all the peaks are shifted toward lower temperatures. Such a shift has already been reported to occur (29, 30) for supported ruthenium sulfide with respect to the bulk reference. These three differences can be related to the smaller particle size and larger surface area of NbS_3-D (18 m^2/g) compared to that of NbS_2 (2 m^2/g).

The reference NbS_2. The TPR curve of NbS_2 (Fig. 3b) shows the existence of three peaks (Table 3). As in the case of NbS_3, the first peak corresponds to surface sulfur. It is less important for NbS_2 than for NbS_3, because the particle size is larger due to the higher preparation temperature. In addition, the crystallite morphologies are different (platelets for NbS_2, needles for NbS_3), which can also contribute to the difference in the surface-sulfur amounts. The second peak observed for NbS_3 (800 K) is missing on the NbS_2 curve, which is to be expected, since this peak is due to the transition from the trisulfide to the nonstoichiometric disulfide $Nb_{1.14}S_2$ (4, 28). As for the second and third peaks of the NbS_2 TPR curve, they unambiguously correspond to the third unresolved peak of NbS_3, and represent the removal of bulk sulfur from the disulfide, with final formation of a metal-rich sulfide of formula $Nb_{1+x}S_2$.

Carbon-supported samples: The role of the sulfurization temperature (T_{sulf}), as shown by the TPR curves (Fig. 3c). First it must be pointed out that for the three supported samples the total amount of sulfur removed per niobium atom (2.6, 2.7, and 1.7 for T_{sulf} = 400, 500, and 600°C, respectively) is larger than for the unsupported reference materials in the same temperature range (Table 3), which can be due to smaller particle size and poorer crystalline organization. The curves obtained for the supported samples exhibit several contributions which can hardly be separated due to overlapping. However, from the simple qualitative comparison of the curves obtained

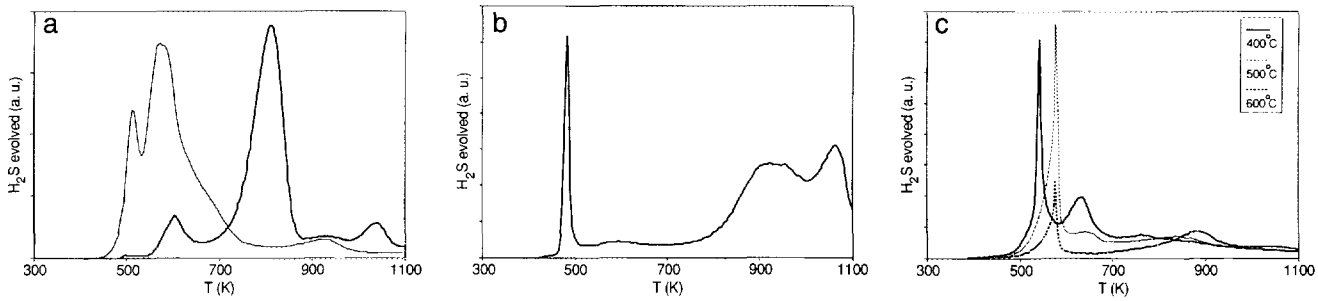

FIG. 3. TPR curves for unsupported niobium sulfides, (a) NbS_3 (heavy line) and NbS_3-D (light line), (b) NbS_2, and (c) for three carbon-supported samples sulfurized at different temperatures.

for increasing T_{sulf} values (400, 500, and 600°C), it can be seen that:

(i) The first peak (surface sulfur) shifts toward higher temperatures (T_{sulf} = 500°C), and its intensity severely decreases (T_{sulf} = 600°C). The temperature shift of this peak indicates that when T_{sulf} is increased it becomes more difficult to remove surface sulfur, which means that the crystalline organization becomes better, as could be expected. As for the intensity decrease, it shows that the surface-sulfur amount diminishes, due of course to the increase in the particle size, as could also be expected.

(ii) The second peak observed for T_{sulf} = 400°C diminishes in intensity (T_{sulf} = 500°C), and vanishes (T_{sulf} = 600°C). From the temperature at which it occurs, this peak can be considered to denote the existence of NbS_3-like species. Their amount thus decreases when T_{sulf} increases, as will be confirmed by the variation in the following peak with T_{sulf}.

(iii) The third peak (or shoulder) observed at about 750 K for T_{sulf} = 400°C shifts toward higher temperatures and becomes more intense. This peak probably corresponds to NbS_2-like entities. As T_{sulf} is increased, these species become more numerous as shown by the greater intensity of the peak, and improve their crystalline organization, which shifts the sulfur-removal temperature.

The increase in the sulfurization temperature T_{sulf} above 400°C accordingly has two sorts of consequence which perfectly explain the concomitant decrease of the catalytic activity.

—The first consequence is morphological: for higher T_{sulf}, the crystalline organization becomes better and the particle size larger, which can only reduce the activity.

—The second consequence is chemical: at T_{sulf} = 400°C, the prepared niobium sulfide mainly corresponds to NbS_3-like species and, when T_{sulf} is increased, these species are replaced by NbS_2-like ones. This chemical evolution is consistent with the behavior observed for unsupported nio-

TABLE 3

Temperature-Programmed Reduction of Unsupported Niobium Sulfides, NbS_3, NbS_3-D, and NbS_2: Peak Temperature, and Corresponding H_2S Production and Formula of the Solid

Starting compound	Peak temperature (K)	H_2S production (mol of S per mol of Nb)	Formula of the solid
NbS_3	600	0.14	$NbS_{2.86}$
	800	1.11	$NbS_{1.75}(Nb_{1.14}S_2)$
	920	0.07	$NbS_{1.68}(Nb_{1.19}S_2)$
	1050	0.07	$NbS_{1.61}(Nb_{1.24}S_2)$
NbS_3-D	520	0.38	$NbS_{2.62}$
	600	1.11	$NbS_{1.51}(Nb_{1.32}S_2)$
	940	0.14	$NbS_{1.43}(Nb_{1.40}S_2)$
NbS_2	480	0.07	$NbS_{1.93}(Nb_{1.03}S_2)$
	920	0.28	$NbS_{1.65}(Nb_{1.21}S_2)$
	1050	0.12	$NbS_{1.53}(Nb_{1.50}S_2)$

TABLE 4

Comparison of the HDS Activities of Supported Molybdenum Sulfide and Niobium Sulfide (10 wt% Metal Loading)

Catalyst	Nb/C	Mo/C	Mo/Al_2O_3
A(HDS) (10^{-8} mol/s g)	110	82	27

bium sulfides: NbS_3 is obtained at lower temperature than NbS_2 and, when heated, it loses sulfur and transforms into nonstoichiometric disulfide. It has already been shown for unsupported samples that the disulfide is less active than the trisulfide. Consequently, the chemical evolution of our supported catalysts also contributes to the activity decrease observed for T_{sulf} values higher than 400°C.

Conclusion

Using the carbon support, which is known to establish weak interactions with active cations, conventional methods allow niobium to be sulfurized and interesting catalytic activities to be reached. For comparison, supported MoS_2 samples have been prepared using "Norit RX3" carbon and γ-alumina. For similar metal loading (10% of the support mass), our best niobium sulfide catalysts are more active than these reference materials (Table 4). On oxide supports, as indicated above, niobium could not be sulfurized under the same conditions, and no catalytic activity could be detected. Here can be found a clear illustration of the support effects: if the cation is somewhat difficult to sulfurize, a support which establishes weak interactions allows the sulfurization to be achieved, whereas a support which establishes stronger interactions does not.

Alumina-Supported Niobium Sulfide Catalysts

For alumina-supported samples prepared under the same conditions as described above for the carbon-supported samples, no Nb–S contribution can be detected by EXAFS in the radial distribution function. This shows that the sulfurization procedure is inefficient, which explains the very poor activity which we measured for such samples. It might be thought that more severe sulfurization routes could be efficient for alumina-supported niobium sulfide to be prepared. First, the Ellingham diagram (31) shows that carbon disulfide CS_2 is, thermodynamically speaking, a better sulfurizing agent than H_2S, up to 1300°C. Moreover, since CS_2 is liquid at room temperature, it can be easily introduced into a high-pressure vessel in order to perform the treatment under pressure. Such a method was already used for the sulfurization of various cations, starting from salts, oxides, or hydroxides as precursors (32, 33), and has been shown to be efficient even at moderate temperature ($T < 500$°C). It thus appears to be particularly convenient for cations which are difficult to sulfurize. For this reason, we have performed sulfurizations with CS_2 in a high-pressure vessel, using alumina as the support and niobium oxalate as the precursor. We introduced into the vessel an excess of liquid CS_2 with respect to the amount required for total transformation of the precursor into NbS_3; then the temperature was raised in the range 350 to 500°C under nitrogen. Under these conditions, the pressure inside the vessel was ca 40 bars.

Optimization of the Sulfurization Treatment

As in the case of carbon-supported niobium sulfide catalysts, the sulfurization treatment was optimized on the basis of the activities measured for the different samples in the reaction of thiophene hydrodesulfurization. For a treatment duration of 4 h, the activity first increases with the sulfurization temperature T_{sulf}, up to 400°C. A higher value of T_{sulf} (450°C) does not improve the activity (Fig. 4a). The influence of the sulfurization duration was then studied for $T_{sulf} = 400$°C (Fig. 4b). The activity first increases, for up to 10 h, and then decreases. The maximum activity obtained under these conditions is significantly higher than that of the reference MoS_2/Al_2O_3 (27×10^{-8} mol/g·s) and the stability in the presence of the reactants is comparable.

Characterization

X-Ray Diffraction

In contrast to the carbon-supported compounds, these alumina-supported catalysts are not completely amorphous to X-ray diffraction. However, only one broad and weak line appears in the diffraction patterns. For $T_{sulf} = 450$°C and for the 100-h sulfurization at 400°C, this line (5.93 Å) corresponds to NbS_2. For shorter treatments at $T_{sulf} = 400$°C, the line is observed at a lower distance (5.75 Å) and can then be attributed to $Nb_{1-y}S$. This compound can be described (34) as a layered MS_2 structure in which the van der Waals space accommodates a large metal excess ($Nb_{1+x}S_2$, with x nearly equal to 1). In this structure, the niobium cations are associated in triangular clusters with Nb–Nb distances (2.92 Å) shorter than the distance between paired niobiums in NbS_3 (3.04 Å). However, one line in a diffraction pattern is not enough and other information, derived for instance from EXAFS experiments, is needed for the active phases to be unambiguously identified.

EXAFS Study

EXAFS measurements at the Nb*K*-edge clearly show that niobium has been sulfurized: the first peak in the radial distribution function (Fig. 5) can be reproduced with an interatomic (corrected) distance of 2.50 Å, which corresponds to Nb–S bonds. A second peak, Nb–Nb, is also

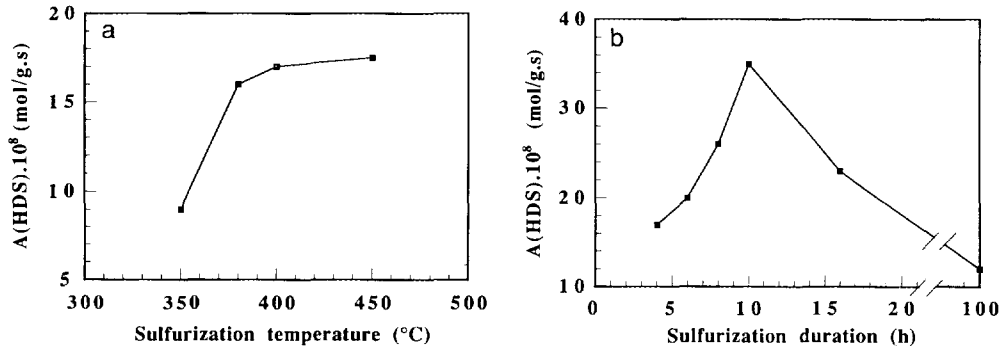

FIG. 4. Variation in the HDS activity of alumina-supported niobium sulfide catalysts with the conditions of sulfurization: (a) temperature and (b) duration.

observed on the RDF's (Fig. 5), and can be used to establish the nature of the Nb–S species. For T_{sulf} = 400°C the second peak appears as a shoulder of the first peak for the shorter sulfurization durations (up to 8 h) and for longer treatments (13 and 16 h) its intensity increases. This peak is related to the existence of a Nb–Nb (corrected) distance of 2.92 Å, which exists precisely in $Nb_{1-y}S$. For the longest treatment (100 h) at T_{sulf} = 400°C, and for T_{sulf} = 450°C, the Nb–Nb peak is shifted toward higher distances. In this case, the (corrected) Nb–Nb distance refines to 3.32 Å, which corresponds to NbS_2-like entities. EXAFS thus unambiguously confirms the structural hypothesis derived from the unique line of the X-ray diffraction patterns.

It must be emphasized that interesting activities are reached even though the active phase ($Nb_{1-y}S$) corresponds to an incomplete sulfurization. The activity of these $Nb_{1-y}S$-like species can possibly be related to the existence of niobium clusters. These metal–metal bonds may be present intrinsically in the catalyst (NbS_3, $Nb_{1-y}S$) or they may occur as an intermediate state during catalysis by NbS_2. In both cases they could act as a reservoir of electrons available for participation in the catalytic reaction.

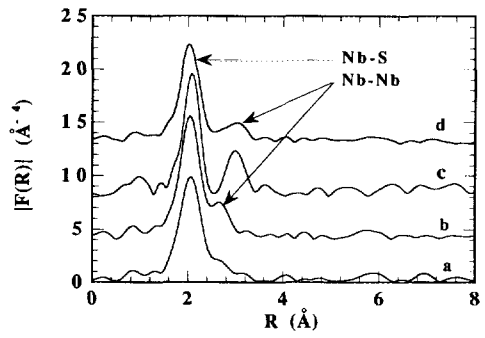

FIG. 5. Radial distribution function at the niobium K-edge for different alumina-supported niobium sulfide catalysts obtained under different sulfurization conditions (temperature and duration): 8 h at 400°C (a), 13 h at 400°C (b), 100 h at 400°C (c), 4 h at 450°C (d).

Electron Microscopy Study

Carbon-supported niobium sulfides are completely amorphous to X rays and their EXAFS peak corresponding to the next-nearest neighbors (Nb–Nb peak) is very weak, which indicates a very poor crystalline organization. Alumina-supported samples can be expected to present a somewhat better organization: one line appears in their diffraction pattern, and the second EXAFS peak is more intense. In order to estimate the crystallinity of our alumina-supported catalysts we examined some samples by transmission electron microscopy. As can be seen in Fig. 6, the niobium sulfide appears as tangled fibers of substantial length and stacking. It can then be anticipated that significant enhancement of the catalytic activity could be obtained insofar as the dispersion of the active phase could be improved.

Is the Sulfurization Method Responsible for the Poor Dispersion of the Active Phase?

It might be thought that the poor dispersion of the active phase is due to the particularity of the sulfurization method (unusual sulfurizing agent, high pressure). In order to estimate the validity of such a hypothesis we decided to compare two alumina-supported catalysts obtained through two different sulfurization methods; namely a conventional method (N_2/15% H_2S at 400°C under atmospheric pressure) and the method reported here for alumina-supported niobium sulfides (CS_2 at 400°C in a high-pressure vessel). This comparison cannot be made effectively with niobium catalysts since the conventional sulfurization routes are in this case inefficient. For this reason we chose to study the influence of the sulfurization method on molybdenum disulfide. The two samples we prepared exhibit exactly the same activity for thiophene hydrodesulfurization (27×10^{-8} mol/g·s) and their morphologies are very similar (Fig. 7), which shows that, at least for molybdenum, sulfurization by CS_2 does not impede formation of a good

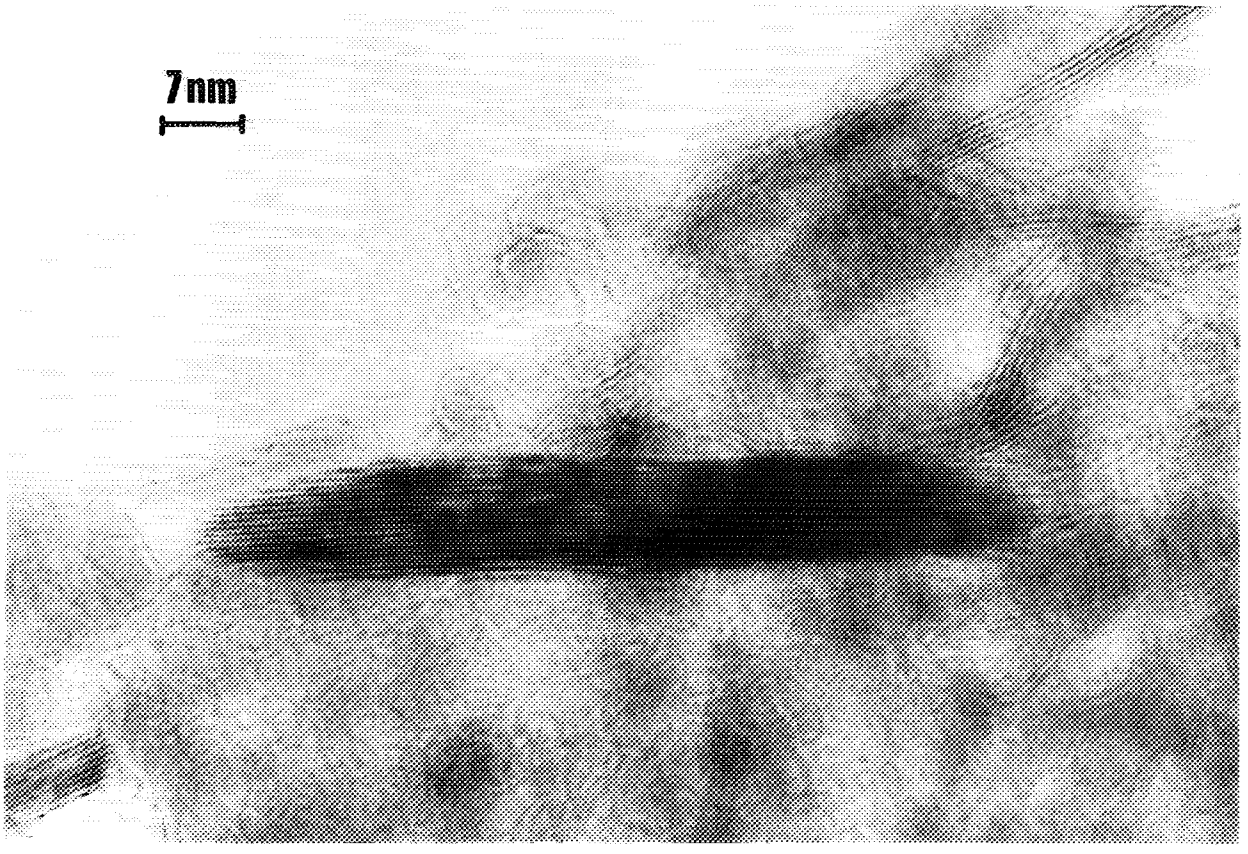

FIG. 6. Transmission electron micrograph of alumina-supported $Nb_{1-y}S$-like domains.

dispersion. This can be thought to be true also for niobium. In this case other experimental parameters (nature of the precursor salt, impregnation and drying methods, etc.) must be considered as possibly responsible for the poor dispersion of alumina-supported niobium sulfide. We plan to perform a systematic study of all these parameters in order to improve the dispersion of the active phase and the catalytic activity. Effectively, it represents an important challenge since despite their poor dispersion, our catalysts surpass the reference MoS_2. These results show that niobium can be sulfurized even on oxide supports, provided a severe sulfurizing route is used. The resulting activities are lower than those of our carbon-supported samples, but higher than that of alumina-supported MoS_2.

CONCLUSION

Since unsupported niobium sulfides were found to be highly effective catalysts for hydrogenolysis reactions, it was necessary for further developments to increase the dispersion of this new active phase by using a support. Experiments clearly indicated that conventional supports such as alumina or silica strongly interact with the active cation and prevent its sulfurization by the usual methods. In order to reduce these interactions, carbon was then used as the support. Active catalysts were obtained and characterized by TPR and EXAFS. The supported entities were found to be NbS_2- and NbS_3-like domains, depending on the sulfurization temperature. The support has been found to influence the dispersion and form of classical MoS_2-based catalysts (35–37), but in the case of niobium this effect is much more drastic since sulfurization cannot be achieved in the usual manner on oxide supports. However, the use of these conventional supports is possible if strong sulfurizing agents are used. Carbon disulfide can also conveniently provide a sulfurized state of the niobium sufficient for it to be an active catalyst. On the alumina support, the active phase was found to be $Nb_{1-y}S$- or NbS_2-like entities, depending on the temperature and duration of the sulfurization treatment. $Nb_{1-y}S$-like species were never observed on the carbon support, and NbS_3-like entities, for which there was evidence in the case of the carbon support, were never found to occur in the alumina-supported catalysts. These differences can be due to the use of different sulfurizing

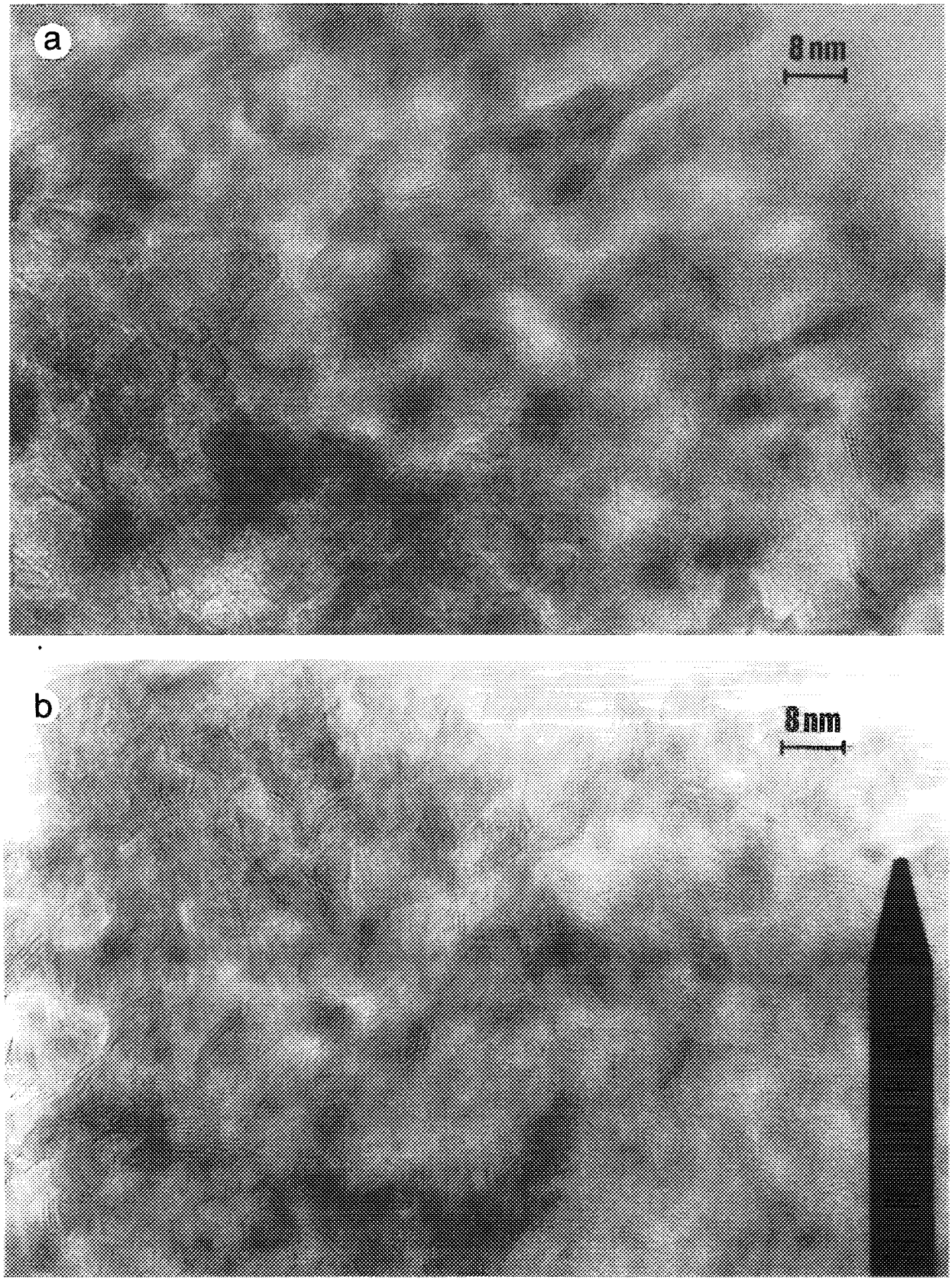

FIG. 7. Transmission electron micrograph of alumina-supported molybdenum sulfide catalysts sulfurized at 400°C by (a) $N_2/15\%H_2S$ under atmospheric pressure, and (b) CS_2 in a high-pressure vessel.

agents and/or to the interactions between the support and the active cation, which can largely affect the chemical behavior of niobium.

ACKNOWLEDGMENTS

This work was carried out in the framework of the contract "Hydrogenation of Aromatic Compounds." The program received support from ELF, IFP, and TOTAL, and from the CNRS (ECOTECH). The authors thank Eric Prouzet and Annie Leblanc for EXAFS data collection and processing.

REFERENCES

1. Pecoraro, T. A., and Chianelli, R. R., *J. Catal.* **67,** 430 (1981).
2. Lacroix, M., Boutarfa, N., Guillard, C., Vrinat, M., and Breysse, M., *J. Catal.* **120,** 473 (1989).
3. Lewis, D. A., and Kenney, C. N., *Trans. Inst. Chem. Eng.* **59,** 186 (1981).
4. Vrinat, M., Guillard, C., Lacroix, M. Breysse, M., Kurdi, M., and Danot, M., *Bull. Soc. Chim. Belg.* **96,** 1017 (1987).
5. Danot, M., Afonso, J., Portefaix, J. L., Breysse, M., and des Courières, T., *Catal. Today* **10,** 629 (1991).
6. Breysse, M., des Courières, T., Danot, M., Geantet, C., and Portefaix, J. L., U.S. Patent 5,157,009, October 20, 1992.
7. Rijnsdorp, J., and Jellinek, F., *J. Solid State Chem.* **25,** 325 (1978).
8. Breysse, M., Afonso, J., Lacroix, M., Portefaix, J. L., and Vrinat, M., *Bull. Soc. Chim. Belg.* **100,** 923 (1991).
9. Ledoux, M. J., Michaux, O., Agostini, G., and Panissod, P., *J. Catal.* **102,** 275 (1986).
10. Rodin, V. N., Startsev, A. N., Zaikovskii, V. I., and Yermakov, Yu. I., *React. Kinet. Catal. Lett.* **32**(2), 419 (1986).
11. Hillerova, E., Sedlaček, J., and Zdrazil, M., *Collect. Czech. Chem. Commun.* **52,** 1748 (1987).
12. Prada Silvy, R., Grange, P., Delannay, F., and Delmon, B., *Appl. Catal.* **46,** 113 (1989).
13. Callant, M., Grange, P., Holder, K. A., Viehe, H. G., and Delmon, B., *J. Catal.* **142,** 725 (1993).
14. De Los Reyes, J. A., Gobolos, S., Vrinat, M., and Breysse, M., *Catal. Lett.* **5,** 17 (1990).
15. Geantet, C., Gobolos, S., De Los Reyes, J. A., Cattenot, M., Vrinat, M., and Breysse, M., *Catal. Today* **10,** 665 (1991).
16. De Los Reyes, J. A., Vrinat, M., Geantet, C., Breysse, M., and Grimblot, J., *J. Catal.* **142,** 455 (1993).
17. Zdražil, M., *Catal. Today* **3**(4), 279 (1988).
18. Kurdi, M., Ph.D. Thesis, Université de Nantes, 1988.
19. Lytle, F. W., Sayers, D. E., and Stern, E. A., *Phys. Rev. B* **11,** 4825 (1975).
20. Stern, E. A., Sayers, D. E., and Lytle, F. W., *Phys. Rev. B* **11,** 4836 (1975).
21. Jones, A., and McNicol, B. D., *in* "Temperature-Programmed Reduction for Solid Materials Characterization." Dekker, New York, 1986.
22. Nag, N. K., Fraenkel, D., Moulijn, J. A., and Gates, B. C., *J. Catal.* **66,** 162 (1980).
23. Burch, R., and Collins, A., *Appl. Catal.* **18,** 373 (1985).
24. Scheffer, B., Dekker, N. J. J., Mangnus, P. J., and Moulijn, J. A., *J. Catal.* **121,** 31 (1990).
25. Guerchais, J. E., and Rohmer, R., *C.R. Acad. Sci. Paris* **259,** 394 (1964).
26. Krishnamurty, K. V., and Harris, G. M., *Chem. Rev.* **61,** 213 (1961).
27. Leblanc, A., Danot, M., Bénazeth, S., and Dexpert, H., *Eur. J. Solid State Inorg. Chem.* **27,** 725 (1990).
28. Kurdi, M., Marie, A. M., and Danot, M., *Solid State Commun.* **64**(4), 395 (1987).
29. De Los Reyes, J. A., Ph.D. Thesis, Université Claude Bernard, Lyon, 1991.
30. Yuan, S., Ph.D. Thesis, Université Claude Bernard, Lyon, 1992.
31. Ellingham, H. J. T., *J. Soc. Chem. Ind.* **63,** 125 (1944).
32. Le Rolland, B., Ph.D. Thesis, Université de Nantes, 1991.
33. Colombet, P., Molinié, P., and Spiesser, M., EP 440 516 A1 (to Rhône Poulenc Chimie, August 7, 1991); *Chem. Abstr.* **115,** 186357-t (1991).
34. Kadijk, F., Ph.D. Thesis, University of Groningen, 1969.
35. Breysse, M., Portefaix, J. L., and Vrinat, M., *Catal. Today* **10,** 489 (1991).
36. Luck, F., *Bull. Soc. Chim. Belg.* **100,** 801 (1991).
37. Delmon, B., *Catal. Lett.* **22,** 1 (1993).